Canonical Wnt signaling inhibits osteoclastogenesis independent of osteoprotegerin

Joachim Albers, Johannes Keller, Anke Baranowsky, Frank Timo Beil, Philip Catala-Lehnen, Jochen Schulze, Michael Amling, and Thorsten Schinke

Department of Osteology and Biomechanics, University Medical Center Hamburg Eppendorf, Hamburg 20246, Germany

Although Wnt signaling is considered a key regulatory pathway for bone formation, inactivation of β-catenin in osteoblasts does not affect their activity but rather causes increased osteoclastogenesis due to insufficient production of osteoprotegerin (Opg). By monitoring the expression pattern of all known genes encoding Wnt receptors in mouse tissues and bone cells we identified Frizzled 8 (Fzd8) as a candidate regulator of bone remodeling. *Fzd8*-deficient mice displayed osteopenia with normal bone formation and increased osteoclastogenesis, but this phenotype was not associated with impaired Wnt signaling or Opg production by osteoblasts. The deduced direct negative influence of canonical Wnt signaling on osteoclastogenesis was confirmed in vitro and through the generation of mice lacking β-catenin in the osteoclast lineage. Here, we observed increased bone resorption despite normal Opg production and a resistance to the anti-osteoclastogenic effect of Wnt3a. These results demonstrate that Fzd8 and β-catenin negatively regulate osteoclast differentiation independent of osteoblasts and that canonical Wnt signaling controls bone resorption by two different mechanisms.

Introduction

Bone remodeling is a continuous process mediated by two cell types, bone-forming osteoblasts and bone-resorbing osteoclasts (Harada and Rodan, 2003; Teitelbaum and Ross, 2003). Understanding the mechanisms controlling their differentiation and/or function is of utmost clinical importance, especially in the context of osteoporosis, a highly prevalent disorder caused by a relative increase of bone resorption over bone formation. Given the fact that therapeutic options for the treatment of osteoporosis are still limited, it is especially important to identify novel targets that can be used to develop specific agonists or antagonists, either blocking bone resorption or activating bone formation. In this regard it was of hallmark importance that two regulatory pathways have been identified over the last years that play crucial roles in the control of bone remodeling. In terms of osteoclast differentiation one of the most relevant factors is the cytokine Rankl, whose deficiency in mice and humans causes osteopetrosis (Boyle et al., 2003). The binding of Rankl to its receptor Rank can be physiologically inhibited by its decoy receptor osteoprotegerin (Opg), whose inactivation causes excessive bone resorption (Bucay et al., 1998). In terms of bone formation, Wnt signaling appears to be one of the most important regulatory pathways, which was first hypothesized based on the finding that inactivating mutations of the Wnt coreceptor low-density lipoprotein receptor-related protein 5 (Lrp5) cause osteoporosis, whereas activating mutations result in excessive bone formation (Gong et al., 2001; Boyden et al., 2002; Little et al., 2002).

Ligands of the Wnt family, which play various roles in development and physiology, bind to a heterodimeric complex consisting of a Frizzled (Fzd) receptor and a coreceptor, Lrp5 or Lrp6 (Clevers and Nusse, 2012). Because mutations of the human *LRP5* gene cause osteosclerosis or osteoporosis, respectively, it became evident that Wnt signaling is a relevant pathway regulating bone remodeling, which has been confirmed through the analysis of various mouse models (Baron et al., 2006). For instance, *Lrp5*-deficient mice display low bone formation, and the same phenotype was found in transgenic mice overexpressing Dickkopf-1 (Dkk1), a secreted Wnt signaling antagonist binding to Lrp5 (Kato et al., 2002; Li et al., 2006). Because the majority of Wnt ligands activate a signaling pathway that involves

J. Albers, J. Keller, and A. Baranowsky contributed equally to this paper.

Correspondence to Thorsten Schinke: schinke@uke.uni-hamburg.de

Abbreviations used in this paper: CRD, cysteine-rich domain; Dkk1, Dickkopf-1; Fzd, Frizzled; LiCl, lithium chloride; Lrp5, low-density lipoprotein receptor-related protein 5; Opg, osteoprotegerin; TRAP, tartrate-resistant acid phosphatase.

The Rockefeller University Press $30.00
J. Cell Biol. Vol. 200 No. 4 537–549
www.jcb.org/cgi/doi/10.1083/jcb.201207142

stabilization and nuclear translocation of β-catenin (canonical Wnt signaling), it was also important to study the influence of β-catenin on osteoblast differentiation and function. Here it was found that β-catenin inactivation in mesenchymal progenitor cells causes an arrest of osteoblast differentiation and severe defects of skeletal development (Day et al., 2005; Hill et al., 2005). In contrast, β-catenin inactivation in mature osteoblasts or in terminally differentiated osteocytes did not affect bone formation, but caused a significant increase in osteoclastogenesis, and the opposite phenotype was observed upon osteoblast-specific activation of β-catenin (Glass et al., 2005; Holmen et al., 2005; Kramer et al., 2010). All of these latter phenotypes were molecularly explained by the fact that β-catenin is required to induce the expression of the osteoclastogenesis inhibitor Opg in osteoblasts, thereby demonstrating an indirect influence of canonical Wnt signaling on bone resorption mediated by β-catenin expression in osteoblasts. Moreover, given the striking phenotypic differences caused by Lrp5 or β-catenin inactivation, it has to be concluded that the Lrp5-dependent control of bone formation is not mediated through canonical Wnt signaling.

Another key question is which of the 10 known Fzd receptors are required to regulate Wnt signaling in the context of bone remodeling. Because Fzd proteins are serpentine receptors and therefore belong to the major class of target proteins for currently available drugs, addressing this questions could also be relevant in terms of identifying novel therapeutic options to treat skeletal disorders (Wise et al., 2002; Overington et al., 2006). Using genome-wide expression analysis of primary osteoblasts we have previously identified *Fzd9* as the only *Fzd* gene with differential expression during the early stages of osteoblastogenesis (Albers et al., 2011). Moreover, we found that *Fzd9*-deficient mice display low bone formation and osteopenia, similar to mice lacking Lrp5. Importantly, canonical Wnt signaling was not impaired in *Fzd9*-deficient osteoblasts, and there was no secondary increase in osteoclastogenesis due to reduced Opg production. These results suggested that Fzd9 regulates osteoblast function through noncanonical Wnt signaling pathways, whereas canonical Wnt signaling in osteoblasts has to be controlled by other Fzd receptors.

With the aim to identify such receptors we have monitored the expression of all known *Fzd* genes in various tissues and bone cells. Because we observed high expression levels of *Fzd8* in osteoblasts and osteoclasts, we analyzed the skeletal phenotype of *Fzd8*-deficient mice. Here we observed osteopenia and increased osteoclastogenesis, but no impairment of canonical Wnt signaling or Opg production in osteoblasts, thus suggesting a direct negative influence of canonical Wnt signaling on osteoclast differentiation. To confirm this hypothesis we generated mice specifically lacking β-catenin in the osteoclast lineage, where we observed an Opg-independent increase of bone resorption.

Results

Fzd8 expression in bone cells

To address the question of which of the 10 known *Fzd* genes could be involved in the regulation of bone remodeling, we first performed qRT-PCR to monitor the expression pattern of all genes encoding Wnt receptor components in various mouse tissues and in cultured osteoblasts and osteoclasts (Fig. 1 A). The most striking result obtained from these analyses was that *Fzd8* was highly expressed in both bone-remodeling cell types, whereas its expression was barely detectable at the tissue level. To follow up on this observation we monitored *Fzd8* expression during the course of primary osteoclast and osteoblast differentiation (Fig. 1 B). When compared with the expression of *Fzd9*, *Fzd8* was expressed at higher levels in both bone cell types, and although its expression in osteoblasts increased significantly between day 15 and day 25 of differentiation, we observed a sharp increase between day 1 and day 4 of osteoclastogenesis. The presence of Fzd8 in both bone cell types at the protein level was further confirmed by immunohistochemistry on human bone sections (Fig. 1 C). Taken together, these results raised the possibility that Fzd8 could be involved in the regulation of bone remodeling, which led us to analyze the skeletal phenotype of *Fzd8*-deficient mice.

Bone formation is unaffected in *Fzd8*-deficient mice

The skeletal phenotype of *Fzd8*-deficient mice was analyzed by non-decalcified histology and histomorphometry of spine sections using wild-type littermates as a control. Although we did not detect significant differences between the two groups at 6 wk of age, there was a significant reduction of the trabecular bone volume in *Fzd8*-deficient mice at 24 wk of age (Fig. 2 A), and the same was the case for $Fzd8^{+/-}$ littermates (BV/TV: 11.7 ± 1.5% in $Fzd8^{+/-}$ mice vs. 15.1 ± 1.5% in wild-type controls). Cellular and dynamic histomorphometry revealed that there was no difference between wild-type and *Fzd8*-deficient mice in terms of osteoblast number and bone formation rate (Fig. 2 B). Consistently, mineralization was not impaired in *Fzd8*-deficient primary osteoblast cultures and the same was the case for the response to the noncanonical Wnt ligand Wnt5a (Fig. 2 C). Because Lrp5 deficiency has been reported to cause persistent embryonic eye vascularization and increased serotonin synthesis in the duodenum, we further quantified the number of hyaloid vessels and circulating serotonin concentrations in wild-type and *Fzd8*-deficient littermates, but here we failed to detect significant differences (Fig. S1). Taken together, these results demonstrated that the osteopenia caused by *Fzd8* deficiency is not related to a defect of bone formation.

Increased osteoclastogenesis in *Fzd8*-deficient mice

We next determined osteoclast number and osteoclast surface in 24-wk-old wild-type and *Fzd8*-deficient littermates and observed that both parameters were significantly increased in the latter ones (Fig. 3 A). To address the question of whether this phenotype is explained by impaired Opg production in osteoblasts, we isolated primary osteoblasts and monitored canonical Wnt signaling after Wnt3a administration. By Western blotting using antibodies against phosphorylated Lrp6 and β-catenin, we did not detect any difference between wild-type and *Fzd8*-deficient cells (Fig. 3 B). Consistent with these findings, there

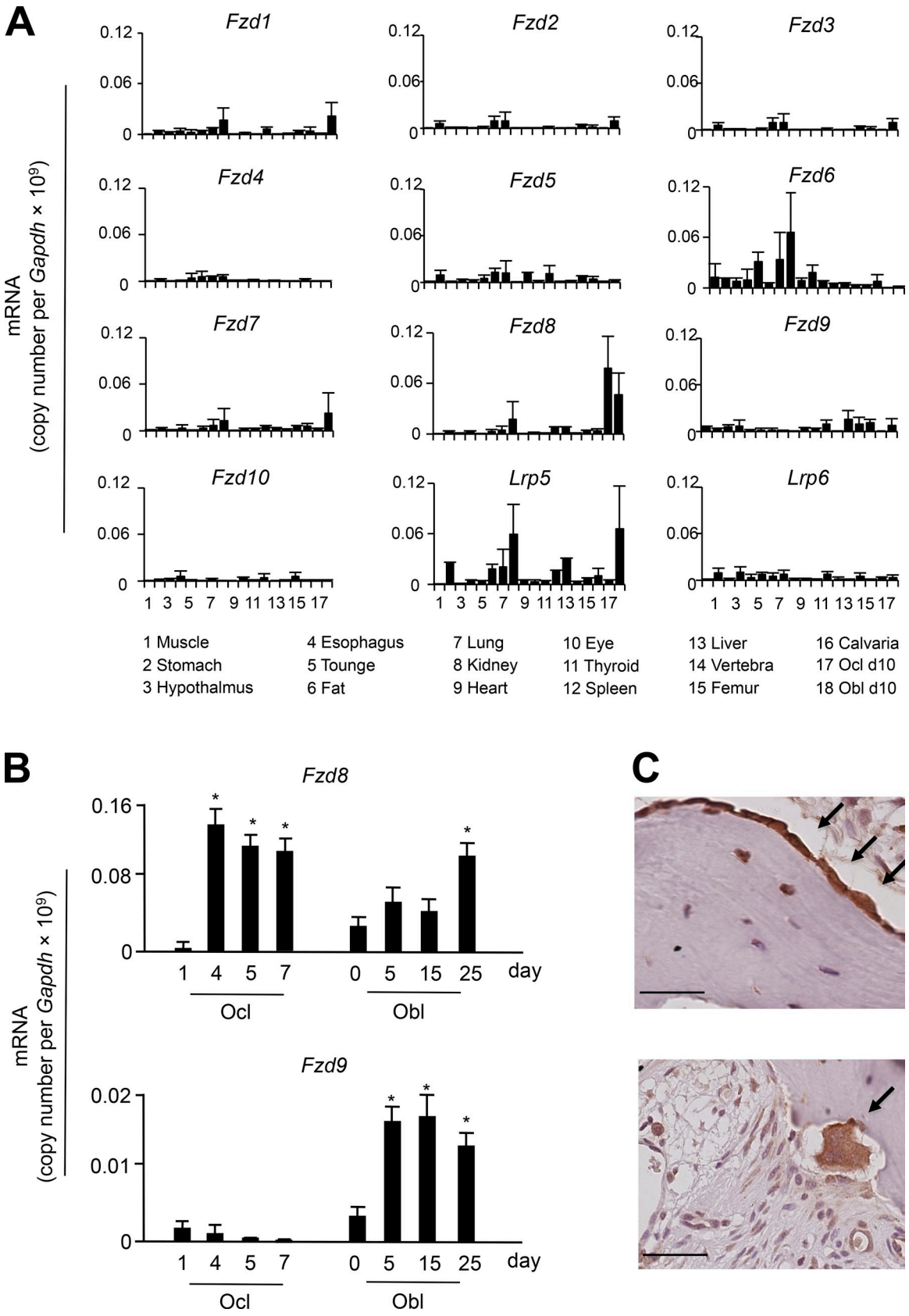

Figure 1. ***Fzd8* expression in bone cells.** (A) qRT-PCR expression analysis for Wnt receptor-encoding genes using cDNA from various tissues and bone cells. Expression levels were normalized to *Gapdh* as indicated. Error bars represent mean ± SD ($n = 4$). (B) qRT-PCR expression analysis for *Fzd8* and *Fzd9* during the course of osteoclast and osteoblast differentiation. Error bars represent mean ± SD ($n = 4$). Asterisks indicate statistically significant differences compared with the earliest stage of differentiation. (C) Immunohistochemistry on human bone sections demonstrates the presence of FZD8 in osteoblasts (top) and osteoclasts (bottom). Bars, 25 μm.

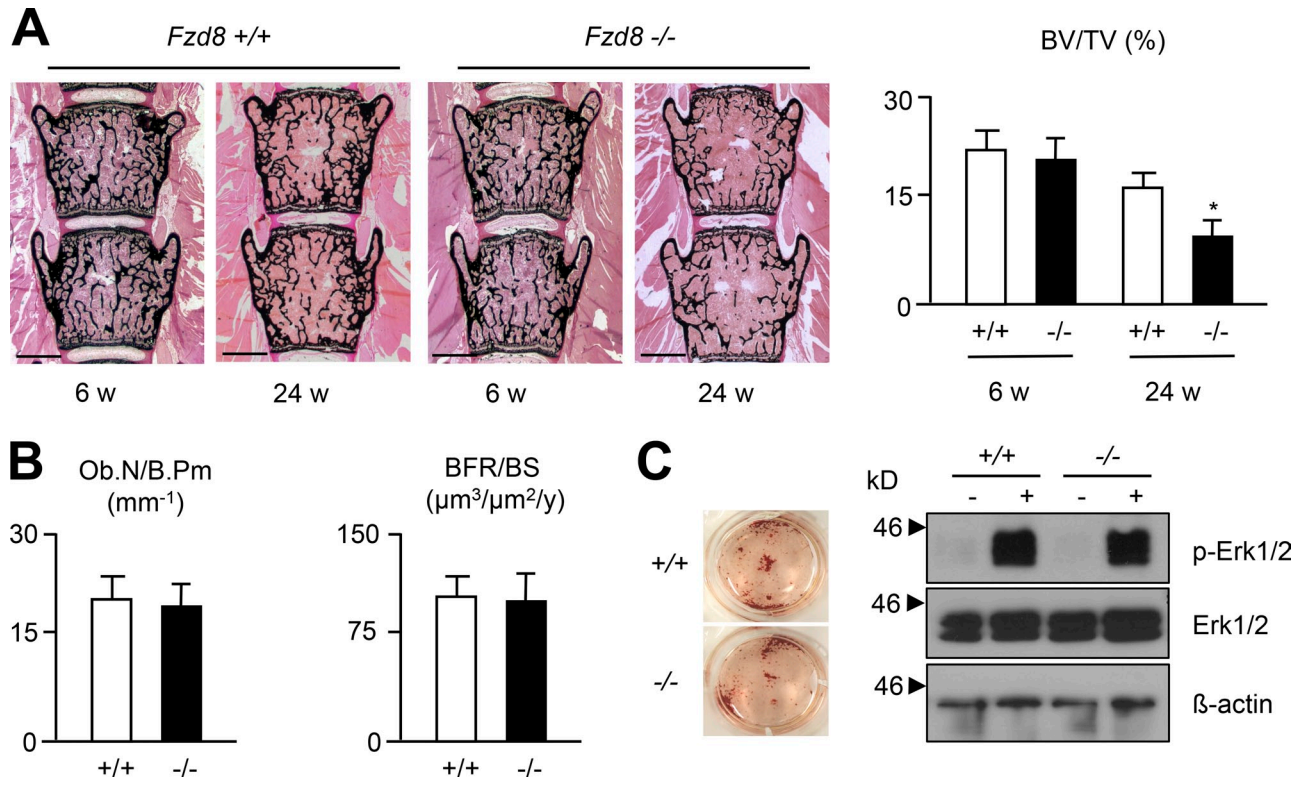

Figure 2. **Phenotypic analysis of *Fzd8*-deficient mice.** (A) Von Kossa/van Gieson staining of spine sections from wild-type and *Fzd8*-deficient mice at the indicated ages. Histomorphometric quantification of the trabecular bone volume (BV/TV) is given on the right. Bars, 1 mm. (B) Quantification of osteoblast number per bone perimeter (Ob.N/B.Pm) and bone formation rate per bone surface (BFR/BS) in 24-wk-old wild-type and *Fzd8*-deficient mice. (C) Alizarin red staining of primary calvarial osteoblasts from wild-type and *Fzd8*-deficient mice after 10 d of differentiation (left) and Western blotting with the indicated antibodies after administration of Wnt5a at day 10 of differentiation (right). The black arrows indicate the position and molecular weight of the nearest marker. All error bars represent mean ± SD (n = 6). Asterisks indicate statistically significant differences between the two groups.

were no significant differences between the two genotypes when we monitored expression of osteoblast differentiation markers or of known target genes of canonical Wnt signaling, such as *Axin2* or *Tnfrsf11b*, the latter one encoding Opg (Fig. 3 C). Most importantly, however, these genes were also expressed at normal rate in bones from *Fzd8*-deficient mice (Fig. 3 D), and there was no significant difference in the serum levels of Rankl and Opg levels between wild-type and *Fzd8*-deficient littermates (Fig. 3 E).

Because these results ruled out a requirement of Fzd8 for canonical Wnt signaling and Opg production in osteoblasts, we next addressed the question of whether the increased osteoclastogenesis observed in *Fzd8*-deficient mice is explained by an osteoblast-independent cell-autonomous defect. For that purpose we isolated bone marrow cells from wild-type and *Fzd8*-deficient mice and differentiated them into osteoclasts ex vivo in the absence or presence of Wnt3a. Here we observed a near complete inhibition of osteoclastogenesis caused by Wnt3a, not only in wild type, but also in *Fzd8*-deficient cultures (Fig. 3 F). Because these findings were not sufficient to demonstrate a cell-autonomous defect of *Fzd8*-deficient osteoclast progenitors, we next performed qRT-PCR to monitor the expression of all genes encoding Wnt receptors. Here we found that none of these were expressed at a higher rate in *Fzd8*-deficient cultures in the absence of Wnt3a, but that all *Fzd* genes, with the exception of *Fzd9*, were significantly overexpressed in these cells in the presence of Wnt3a (Fig. 4 A). Importantly, however, a compensatory induction of other *Fzd* genes in *Fzd8*-deficient mice was not observed in vivo (Fig. 4 B), thus implying that the failure to demonstrate a cell-autonomous defect of *Fzd8*-deficient osteoclasts is potentially explained by a Wnt3a-dependent induction of other *Fzd* genes in *Fzd8*-deficient cultures specifically ex vivo.

Activating canonical Wnt signaling in osteoclast progenitors inhibits their differentiation

Although it was essentially impossible for us to demonstrate a cell-autonomous defect of *Fzd8*-deficient osteoclast progenitors, our results raised the possibility that canonical Wnt signaling has a direct negative influence on osteoclastogenesis, in addition to its known indirect effect by increasing Opg production by osteoblasts. To address this possibility we first analyzed the effects of lithium chloride (LiCl), Wnt3a, and Wnt5a on osteoclast differentiation using wild-type bone marrow progenitor cells. In the first set of experiments we added these three Wnt signaling activators to the medium during the whole course of differentiation (together with 1,25 dihydroxyvitamin-D3), whereas M-Csf and Rankl, according to standard protocols, were only added from day 4 to day 7 of differentiation. By quantifying the number of tartrate-resistant acid phosphatase (TRAP)–positive multinucleated cells we observed a dose-dependent

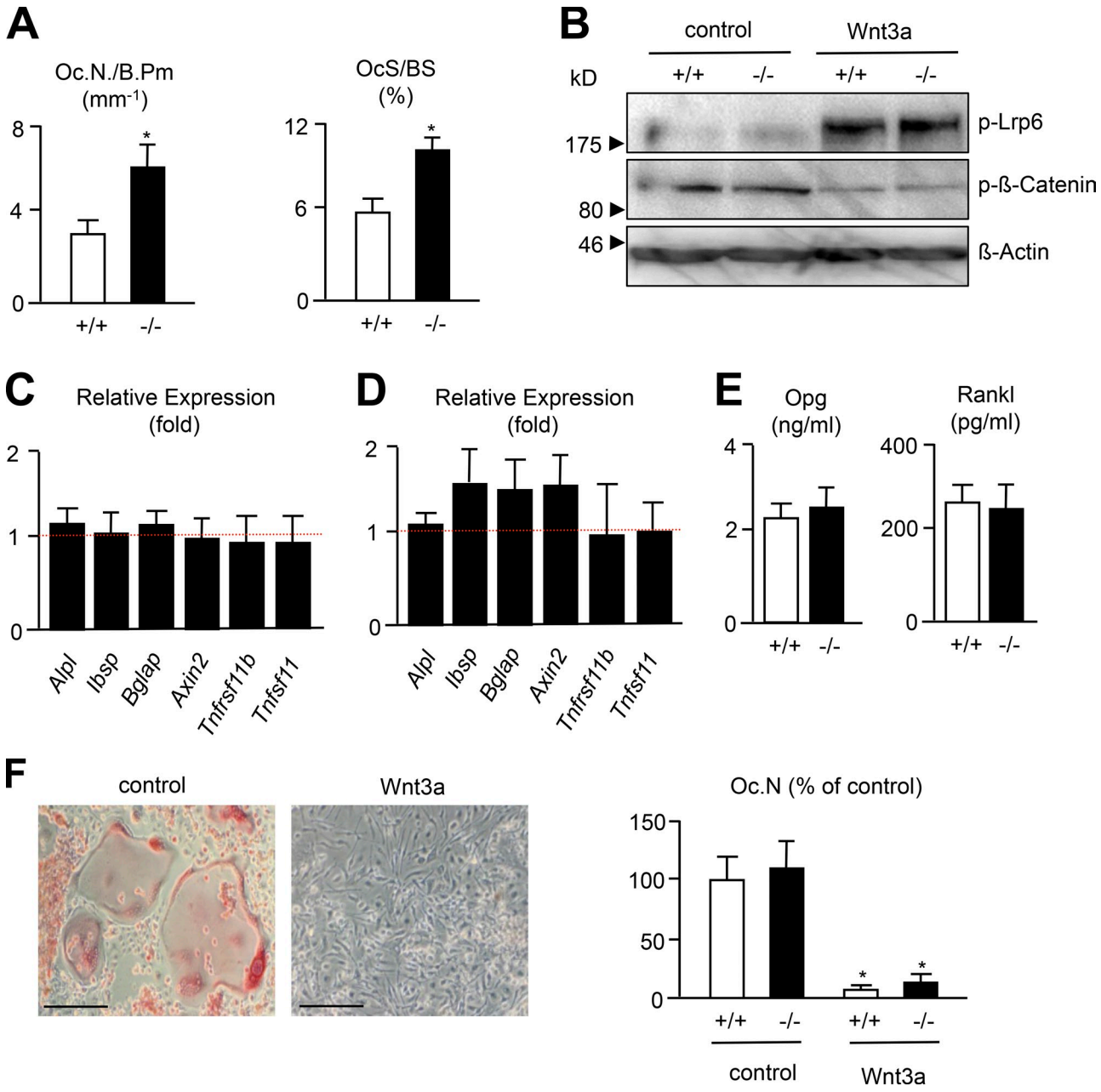

Figure 3. **Increased osteclastogenesis in *Fzd8*-deficient mice.** (A) Quantification of osteoclast number per bone perimeter (Oc.N/B.Pm) and osteoclast surface per bone surface (OcS/BS) in 24-wk-old wild-type and *Fzd8*-deficient mice. Error bars represent mean ± SD (n = 6). Asterisks indicate statistically significant differences between the two groups. (B) Western blot analysis for phosphorylated Lrp6 and β-catenin after stimulation of wild-type and *Fzd8*-deficient osteoblasts by Wnt3a at day 10 of differentiation. The black arrows indicate the position and molecular weight of the nearest marker. (C) qRT-PCR expression analysis of the indicated genes in *Fzd8*-deficient osteoblasts relative to wild-type cultures. Error bars represent mean ± SD (n = 4). (D) qRT-PCR expression analysis of the same genes in *Fzd8*-deficient marrow-flushed bones relative to wild-type littermates. Error bars represent mean ± SD (n = 4). (E) Serum levels of Opg and Rankl in 24-wk-old wild-type and *Fzd8*-deficient littermates. Error bars represent mean ± SD (n = 6). (F) TRAP activity staining of bone marrow cells differentiated in the presence of M-Csf and Rankl with or without Wnt3a as indicated. Bars, 50 µm. Quantification of TRAP-positive multinucleated cells in wild-type and *Fzd8*-deficient cultures is given on the right. Error bars represent mean ± SD (n = 6). Asterisks indicate statistically significant differences compared with control-treated cells.

inhibition of osteoclastogenesis caused by LiCl and Wnt3a, which are both known to activate canonical Wnt signaling in various cell types (Fig. 5 A). In contrast, Wnt5a, a ligand known to activate noncanonical Wnt signaling pathways, did not inhibit, but activated osteoclast differentiation, in line with data published by others (Maeda et al., 2012). Because the induction of *Fzd8* expression during osteoclastogenesis occurs before the addition of M-Csf and Rankl, we next addressed the question of whether the Wnt3a-mediated inhibition of osteoclastogenesis would also occur at an early stage of differentiation, which we did by modifying the timing of Wnt3a and Rankl administration. When both molecules were present during the whole course of differentiation, Wnt3a caused inhibition of osteoclastogenesis, similar to the experiments described above (Fig. 5 B). In contrast,

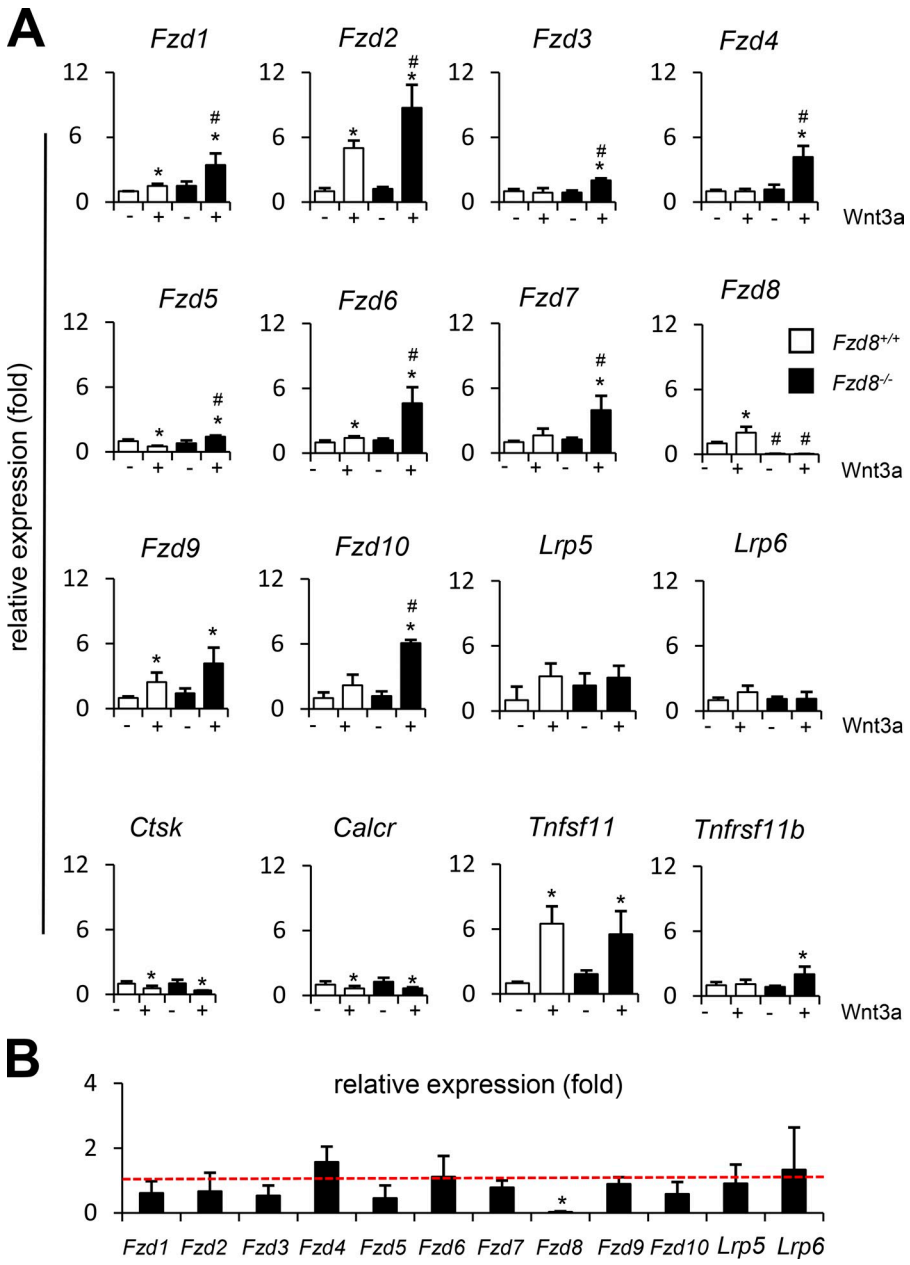

Figure 4. **Compensatory induction of *Fzd* genes in Wnt3a-treated *Fzd8*-deficient osteoclast cultures.** (A) qRT-PCR expression analysis of the indicated genes in wild-type and *Fzd8*-deficient bone marrow cultures differentiated in the presence of M-Csf and Rankl with or without Wnt3a as indicated. Error bars represent mean ± SD (n = 4). Asterisks indicate statistically significant differences compared with control-treated cells. Number signs indicate statistically significant differences between wild-type and *Fzd8*-deficient cultures. (B) qRT-PCR expression analysis of the indicated genes in *Fzd8*-deficient marrow-flushed bones relative to wild-type littermates. Error bars represent mean ± SD (n = 4).

when Wnt3a was only added from day 4 to day 7 of differentiation, it did not mediate an inhibitory defect on osteoclastogenesis, and the effect of LiCl was also reduced (Fig. 5 C).

Based on these findings, we next monitored the effects of Wnt3a on gene expression at day 3 of differentiation and treated the cells with Wnt3a for 6 h to subsequently perform qRT-PCR. Although we did not observe an effect of Wnt3a on the expression of *Ctsk* (encoding Cathepsin K) or *Tnfrsf11a* (encoding Rank), Wnt3a administration resulted in a significant induction of *Axin2* and *Tnfrsf11b* expression, as expected, yet the expression of *Tnfsf11* (encoding Rankl) was induced to the same extent (Fig. 5 C). We additionally applied Western blotting with antibodies against phosphorylated Lrp6 and β-catenin to demonstrate activation of canonical Wnt signaling by Wnt3a in the same cultures, and here we could also observe that this effect is abrogated by the presence of the Fzd8 cysteine-rich domain (CRD; Fig. 5 E), which can be used to block receptor binding (DeAlmeida et al., 2007; Schulte and Bryja, 2007).

We next differentiated the bone marrow progenitor cells in the presence of Wnt3a and/or a monoclonal antibody neutralizing Opg (Glass et al., 2005) and found that Wnt3a significantly reduced osteoclastogenesis also in the presence of the antibody (Fig. 6 A). Moreover, we applied CD11b immunoaffinity to separate CD11b-negative stromal cells from CD11b-positive osteoclast progenitors and analyzed the effects of Wnt3a on the differentiation of the latter ones. Here we found that Wnt3a also inhibited osteoclastogenesis (Fig. 6 B), despite the fact the Opg was undetectable in the medium of the cells, in contrast to unsorted cells, where Opg concentration was above 100 pg/ml. We further analyzed the effects of Wnt3a on gene expression in Cd11b-sorted cultures, and here we did not observe an induction of *Tnfsf11* and *Tnfrsf11b* expression, albeit

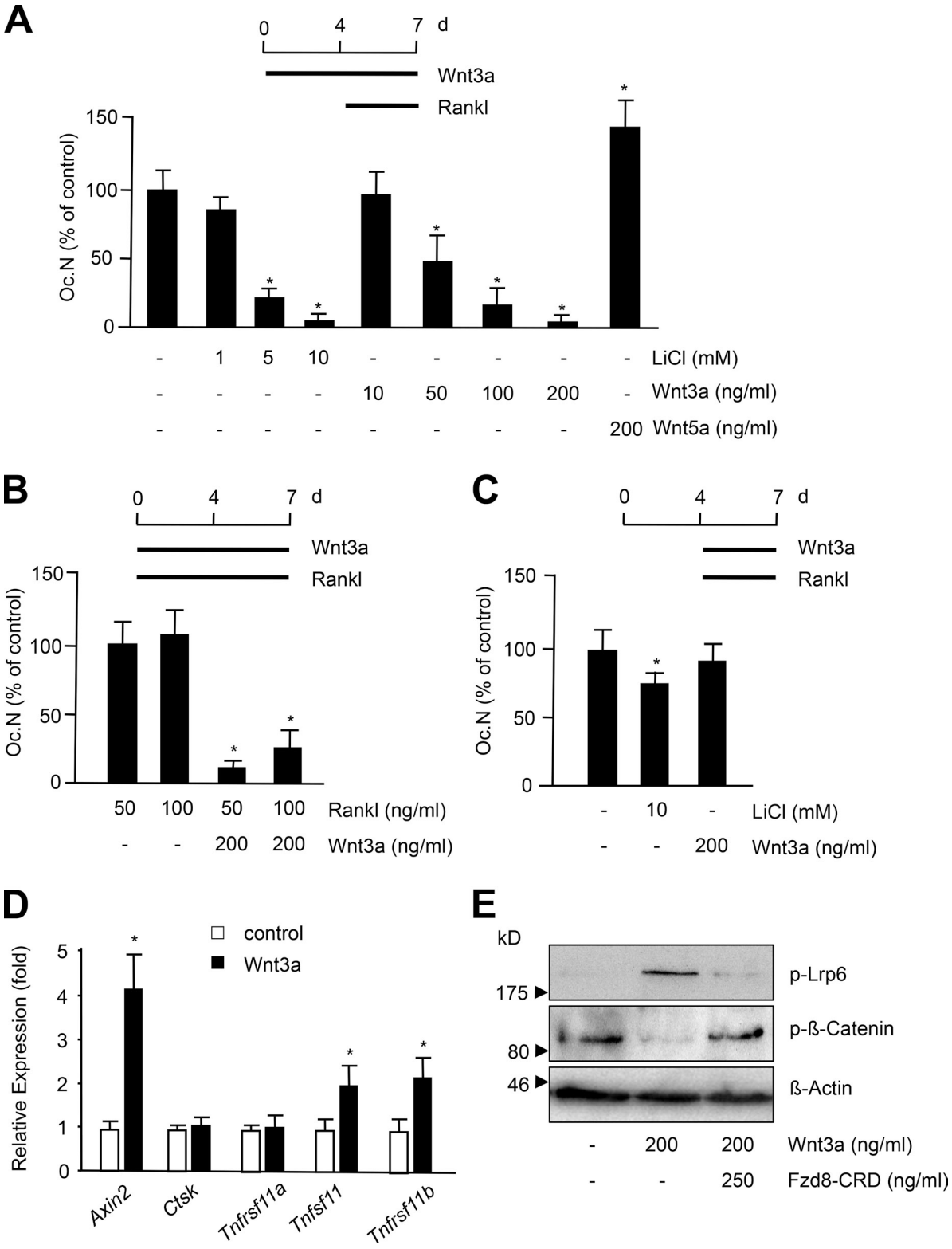

Figure 5. **Inhibition of osteoclastogenesis by canonical Wnt signaling.** (A) Quantification of TRAP-positive multinucleated cells generated in the presence of different concentrations of LiCl, Wnt3a, or Wnt5a as indicated. (B) Quantification of TRAP-positive multinucleated cells generated after 7 d of culture in the permanent presence of recombinant Wnt3a and Rankl as indicated. (C) Quantification of TRAP-positive multinucleated cells generated after 7 d of culture, when Wnt3a (or LiCl) and Rankl were added from day 4 of culture. (D) qRT-PCR expression analysis for the indicated genes in bone marrow cultures at day 3 of differentiation after treatment with 200 ng/ml Wnt3a for 6 h. All error bars represent mean ± SD (n = 6). Asterisks indicate statistically significant differences compared with controls. (E) Western blot analysis for phosphorylated Lrp6 and β-catenin after stimulation of bone marrow cultures at day 3 of differentiation by Wnt3a in the absence or presence of the Fzd8-CRD. The black arrows indicate the position and molecular weight of the nearest marker.

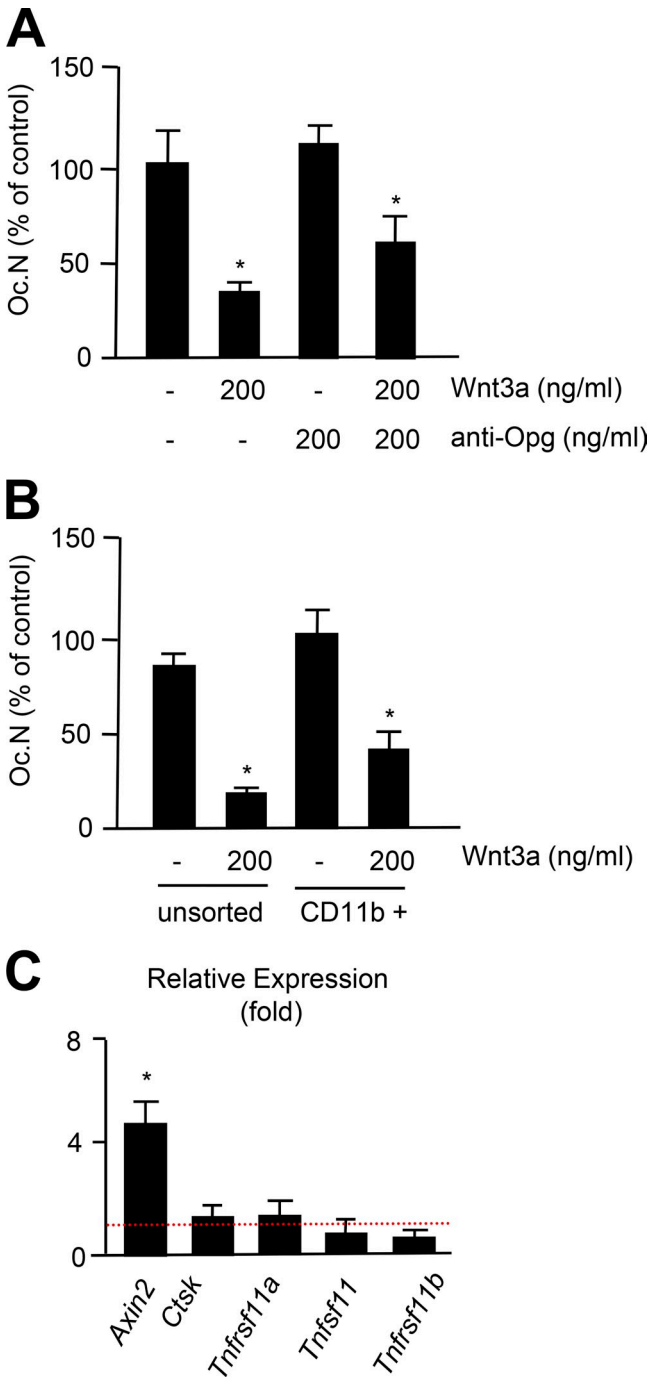

Figure 6. **Opg-independent inhibition of osteoclastogenesis by Wnt3a.** (A) Quantification of TRAP-positive multinucleated cells generated after 7 d of culture in the presence of Wnt3a and/or an anti-Opg antibody. Error bars represent mean ± SD (n = 6). Asterisks indicate statistically significant differences compared with controls. (B) Quantification of TRAP-positive multinucleated cells generated from unsorted or CD11b-purified bone marrow cells after 7 d of culture in the presence of Wnt3a. Error bars represent mean ± SD (n = 6). Asterisks indicate statistically significant differences compared with controls. (C) qRT-PCR expression analysis of the indicated genes in CD11b-purified bone marrow cells after treatment with 200 ng/ml Wnt3a for 6 h relative to untreated cells. Error bars represent mean ± SD (n = 4). Asterisks indicate statistically significant differences compared with controls.

Axin2 expression was increased (Fig. 6 C). Collectively, these results suggested that canonical Wnt signaling negatively regulates osteoclastogenesis independent of Opg, which led us to address the question of whether a specific deletion of β-catenin in cells of the osteoclast lineage would affect bone resorption in vivo.

Mice lacking β-catenin in the osteoclast lineage display increased bone resorption despite normal Opg production by osteoblasts

Here we took advantage of a mouse model carrying loxP sites within the *Ctnnb1* gene that was crossed with transgenic mice expressing the Cre-recombinase under the control of the *LysM* promoter (Clausen et al., 1999; Brault et al., 2001). The resulting $Ctnnb1^{fl/fl}/LysM^{+/cre}$ mice were first monitored for specificity of recombination using genomic PCR from various tissues and primary bone cells, and consistent with the *LysM* expression pattern we observed recombination in spleen and cultured osteoclasts, but not in osteoblasts (Fig. S2 A). Likewise, primary osteoblasts from $Ctnnb1^{fl/fl}/LysM^{+/cre}$ mice mineralized normally (Fig. S2 B), displayed normal *Tnfsf11* and *Tnfrsf11b* expression (Fig. S1 C), and responded to the Wnt3a administration in the same way as $Ctnnb1^{fl/fl}/LysM^{+/+}$ cells (Fig. S1 D). We next analyzed the skeletal phenotype of the $Ctnnb1^{fl/fl}/LysM^{+/cre}$ mice by non-decalcified histology and observed osteopenia at 12 wk of age (Fig. 7 A). Histomorphometry confirmed that $Ctnnb1^{fl/fl}/LysM^{+/cre}$ mice displayed a significant reduction of the trabecular bone volume compared with Cre-negative littermates, whereas the bone formation rate, as well as osteoblast number and surface, were unaffected (Fig. 7 B).

In contrast, TRAP activity staining and cellular histomorphometry revealed that osteoclastogenesis was significantly increased in $Ctnnb1^{fl/fl}/LysM^{+/cre}$ mice (Fig. 8 A), and the same was the case for bone-specific collagen degradation products (Crosslaps) in the serum (Fig. 8 B). Most importantly, however, the serum concentrations of Opg and Rankl were not significantly different between $Ctnnb1^{fl/fl}/LysM^{+/+}$ and $Ctnnb1^{fl/fl}/LysM^{+/cre}$ mice, and *Tnfsf11* and *Tnfrsf11b* expression was unaffected in the latter ones, both in vivo and in vitro (Fig. 8 C). Finally, we analyzed the effects of Wnt3a on osteoclast differentiation from bone marrow progenitor cells of $Ctnnb1^{fl/fl}/LysM^{+/+}$ and $Ctnnb1^{fl/fl}/LysM^{+/cre}$ mice. Here we found that the significant reduction of osteoclastogenesis caused by Wnt3a administration was fully abrogated in $Ctnnb1^{fl/fl}/LysM^{+/cre}$ cultures, thereby demonstrating that these effects depend on the presence of β-catenin (Fig. 8 D). Collectively, our findings provide evidence for a direct inhibitory effect of canonical Wnt signaling on osteoclastogenesis, which is independent from the known indirect effect mediated through β-catenin expression in osteoblasts.

Discussion

Although it is commonly accepted that intact Wnt signaling is essential for proper bone formation and remodeling, there are still many open questions regarding the specific mechanisms involved in this type of regulation, and there is still a controversial

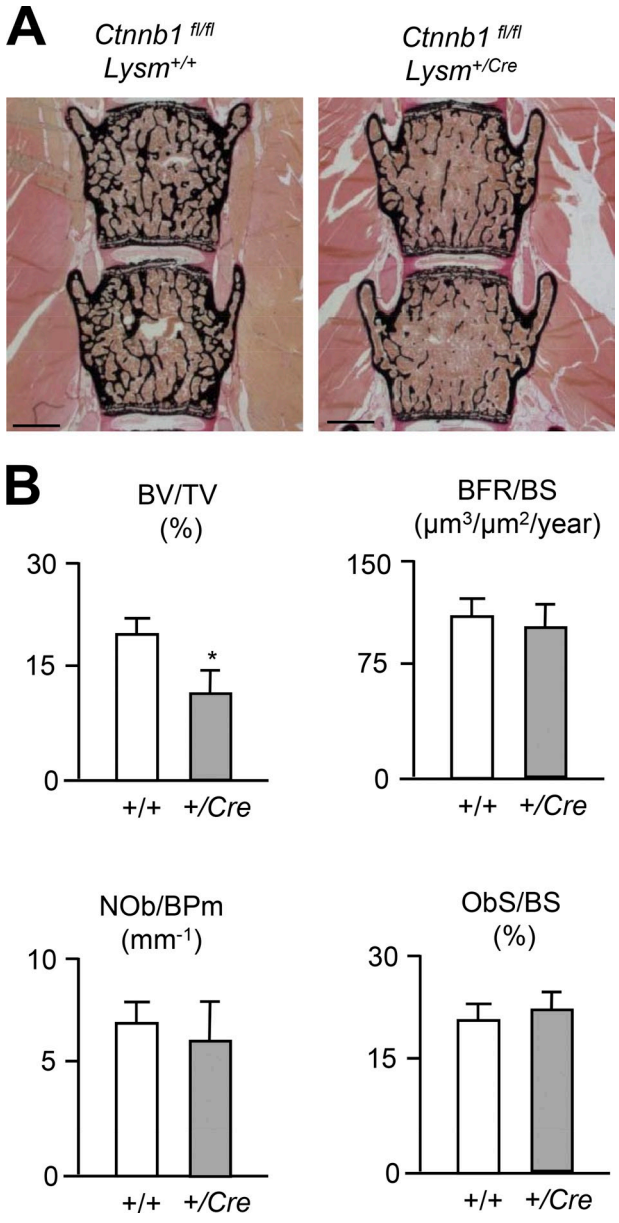

Figure 7. **Phenotypic analysis of *Ctnnb1*$^{fl/fl}$/*LysM*$^{+/cre}$ mice.** (A) Von Kossa/van Gieson-staining of non-decalcified spine sections from 12-wk-old *Ctnnb1*$^{fl/fl}$/*LysM*$^{+/+}$ and *Ctnnb1*$^{fl/fl}$/*LysM*$^{+/cre}$ mice. Bars, 1 mm. (B) Histomorphometric quantification of trabecular bone volume (BV/TV), bone formation rate (BFR/BS), osteoblast number (Ob.N/B.Pm), and osteoblast surface (ObS/BS) in the same mice. All error bars represent mean ± SD (n = 6). Asterisks indicate statistically significant differences between the two groups.

debate regarding the mechanism of Lrp5 action (Yadav et al., 2008; Cui et al., 2011). What is obvious, however, is that ubiquitous inactivation of Lrp5 causes a bone-remodeling phenotype that is fundamentally different from the phenotypes observed in various mouse models with cell type–specific inactivation of β-catenin. More specifically, although β-catenin inactivation in mesenchymal progenitor cells causes severe skeletal defects, because osteoblastogenesis is shifted toward ectopic chondrogenesis, *Lrp5*-deficient mice do not display such defects of skeletal development (Kato et al., 2002; Day et al., 2005; Hill et al., 2005). Likewise, while osteoclastogenesis and Opg production by osteoblasts are unaffected by the absence of Lrp5, β-catenin inactivation in mature osteoblasts does not impair bone formation. This has been demonstrated by three different strategies using *Col1a1-Cre*, *Osteocalcin-Cre*, or *Dmp1-Cre* transgenic mice, and in all cases β-catenin inactivation specifically caused increased bone resorption due to reduced Opg production (Glass et al., 2005; Holmen et al., 2005; Kramer et al., 2010).

We have previously analyzed two mouse models with impaired Wnt signaling in osteoblasts, mice lacking the Wnt receptor *Fzd9* and mice overexpressing the Dkk1 receptor *Krm2* in osteoblasts. Here we found that *Fzd9* deficiency results in a significant reduction of bone formation without affecting osteoclastogenesis, whereas *Krm2*-transgenic mice display severe osteoporosis caused by both reduced bone formation and increased osteoclastogenesis (Schulze et al., 2010; Albers et al., 2011). Importantly, although primary osteoblasts from *Krm2*-transgenic mice displayed impaired canonical Wnt signaling and *Tnfrsf11b* expression, also resulting in reduced serum levels of Opg, *Fzd9*-deficient osteoblasts responded normally to Wnt3a stimulation, and their cell-autonomous defect was related to a disturbance of noncanonical Wnt signaling pathways. Collectively, these findings demonstrated that canonical Wnt signaling in osteoblasts is not controlled by Fzd9, and that other Fzd receptors are required for the known effects of β-catenin. To identify such a receptor we analyzed the expression pattern of all known *Fzd* genes and subsequently analyzed the impact of *Fzd8* deficiency on bone remodeling because this gene was found highly and differentially expressed in cultured osteoblasts and osteoclasts.

Although *Fzd8*-deficient mice displayed osteopenia due to increased osteoclastogenesis, similar to mice lacking β-catenin in osteoblasts, we were able to rule out that this defect is mediated through impaired Wnt signaling in osteoblasts, and most importantly, there was no reduction of Opg levels in the serum of *Fzd8*-deficient mice. Although we did not observe increased osteoclastogenesis of *Fzd8*-deficient bone marrow cells ex vivo, neither in the absence nor in the presence of Wnt3a, we were able to demonstrate that canonical Wnt signaling inhibits osteoclastogenesis independent of Opg production by osteoblasts, which was finally confirmed through the generation of mice lacking β-catenin in the osteoclast lineage. At that point it is important to state that two other studies have been published at the time of our analysis where *Lysm-Cre* mediated inactivation of β-catenin has been reported to cause osteopenia due to increased osteoclastogenesis (Wei et al., 2011; Otero et al., 2012). However, although both studies provided evidence for a direct inhibitory effect of canonical Wnt signaling on osteoclast formation, they did not demonstrate that β-catenin signaling and Opg production were unaffected in osteoblasts in these mice. Therefore, it is in our opinion important that we could additionally show (1) specificity of recombination in our mouse model, (2) unaffected differentiation and gene expression in primary osteoblasts from these mice, (3) normal Opg serum levels, and (4) abrogation of the inhibitory effect of Wnt3a on osteoclastogenesis. Moreover, we could identify Fzd8 as a negative regulator of bone resorption, at least in vivo, which is particularly relevant because *Fzd8*-deficient mice do not display obvious pathologies elsewhere.

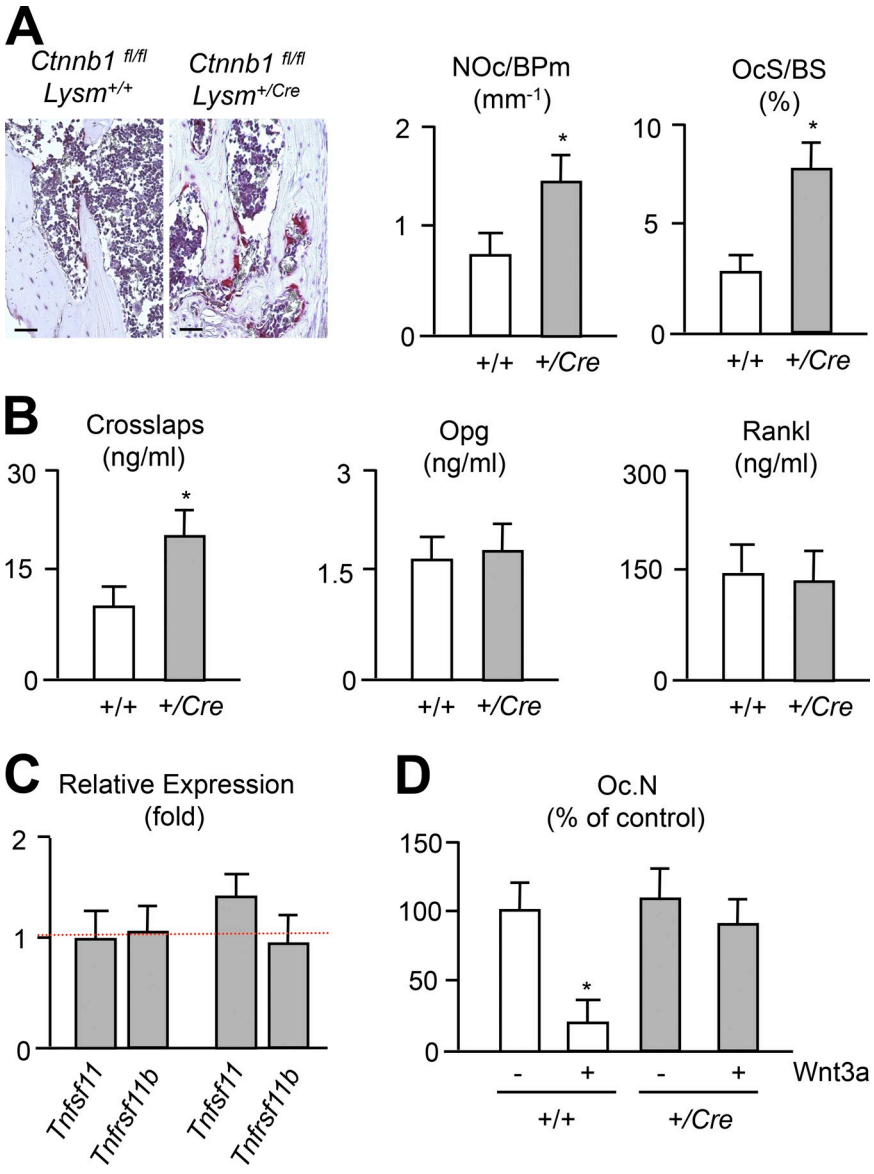

Figure 8. **Opg-independent increase of osteoclastogenesis in *Ctnnb1*$^{fl/fl}$/*LysM*$^{+/cre}$ mice.** (A) TRAP activity staining on spine sections shows increased osteoclastogenesis in *Ctnnb1*$^{fl/fl}$/*LysM*$^{+/cre}$ mice. Histomorphometric quantification of osteoclast number (Oc.N/B.Pm) and osteoclast surface (OcS/BS) is given on the right. Bars, 50 µm. (B) Concentrations of collagen degradation products (Crosslaps), Opg, and Rankl in the serum of *Ctnnb1*$^{fl/fl}$/*LysM*$^{+/+}$ and *Ctnnb1*$^{fl/fl}$/*LysM*$^{+/cre}$ mice. All error bars represent mean ± SD (n = 6). Asterisks indicate statistically significant differences between the two groups. (C) qRT-PCR expression analysis of the indicated genes in marrow-flushed bones (left) or in bone marrow–derived osteoclast cultures (right) from *Ctnnb1*$^{fl/fl}$/*LysM*$^{+/cre}$ mice relative to *Ctnnb1*$^{fl/fl}$/*LysM*$^{+/+}$ littermates. Error bars represent mean ± SD (n = 4). (D) Quantification of TRAP-positive multinucleated cells in *Ctnnb1*$^{fl/fl}$/*LysM*$^{+/+}$ and *Ctnnb1*$^{fl/fl}$/*LysM*$^{+/cre}$ bone marrow cells differentiated by addition of M-Csf, Rankl in the absence of presence of Wnt3a, as indicated. All error bars represent mean ± SD (n = 6). Asterisks indicate statistically significant differences compared with untreated controls.

Despite the fact that we were not able to detect a cell-autonomous defect of *Fzd8*-deficient osteoclasts, likely explained by a compensatory induction of other *Fzd* genes, this latter notion is potentially relevant because Fzd8 is a serpentine receptor, i.e., it belongs to the major class of target proteins for currently available drugs (Wise et al., 2002; Overington et al., 2006). Given the fact that activating Wnt signaling is now considered one of the most promising approaches to treat individuals with osteoporosis, multiple myeloma, or metastatic bone disease (Rachner et al., 2011; Rachner et al., 2012), it is surprising that there is still limited knowledge on the specific roles of Fzd receptors in bone cells. Of note, the Wnt-mediated interaction between osteoblasts and osteoclasts is not only relevant for osteoporosis, but also for the development of osteolytic lesions, particularly in individuals with multiple myeloma. This was first shown by genome-wide expression analysis demonstrating elevated expression of the Wnt antagonist Dkk1 by myeloma tumor cells (Tian et al., 2003). The potential therapeutic relevance of these findings was confirmed in animal experiments, where the administration of either a Dkk1-neutralizing antibody or of recombinant Wnt3a attenuated the development of osteolytic lesions in immunodeficient mice engrafted with multiple myeloma cells (Yaccoby et al., 2007; Qiang et al., 2008; Heath et al., 2009). Therefore, it is conceivable to speculate that Fzd8 might serve as a novel target protein for anti-resorptive treatment of various bone loss disorders. In this regard it can be an advantage that the crystal structure of the Fzd8-CRD has already been characterized (Dann et al., 2001), which could allow in silico design of specific agonists.

Materials and methods

Expression analysis

RNA was isolated from various tissues, marrow-flushed bones, or primary bone cells using the RNeasyMini kit (QIAGEN), and DNase digestion was performed according to the manufacturer's instructions. Concentration and quality of RNA were measured using an ND-1000 system (NanoDrop Technology). For cDNA synthesis, 1 µg of RNA was reverse transcribed using SuperScriptIII (Invitrogen) according to the manufacturer's instructions. qRT-PCR expression analysis was performed using a StepOnePlus system

and predesigned TaqMan gene expression assays (Applied Biosystems). *Gapdh* expression was used as an internal control. Immunohistochemistry was performed on decalcified human bone sections derived from healthy donors at autopsy. After blocking nonspecific binding sites with 2.5% BSA, incubation with an antibody against human FZD8 (#AF2440; R&D Systems) was performed overnight. After incubation with a biotinylated secondary antibody and streptavidin/HRP, peroxidase activity was detected with DAB as a chromogenic substrate.

Primary osteoblasts

Primary osteoblasts were isolated by sequential collagenase digestion and differentiated for 10 d by the addition of 50 µg/ml ascorbic acid and 10 mM β-glycerophosphate. Assessment of mineralization by alizarin red staining was performed as described previously (Albers et al., 2011). In brief, cells were washed with PBS and fixed in 90% ethanol for 1 h. After washing twice with distilled water, cells were stained with alizarin red S solution (40 mM, pH 4.2) for 10 min. After additional washing steps with distilled water, images were taken with a digital camera (EOS 10D; Canon). Quantification was performed by dissolving the cell-bound alizarin red S in 10% acetic acid, incubating for 30 min at room temperature, and for 10 min at 85°C. After a centrifugation step the supernatant was neutralized with 10% ammonium hydroxide solution, and the absorbance was measured at 405 nm. To analyze the response to Wnt ligands cells were serum starved overnight and then stimulated by the addition of Wnt5a (#645WN, 100 ng/ml; R&D Systems) or Wnt3a (#1324WN, 100 ng/ml; R&D Systems). Whereas RNA was isolated after 6 h for qRT-PCR expression analysis, protein extracts were isolated after 30 min by cell lysis with RIPA buffer (1% NP-40, 1% sodium deoxycholate, 0.1% sodium dodecylsulfate, 150 mM sodium chloride, 2 mM EDTA, and 10 mM sodium phosphate) containing a protease and phosphatase inhibitor cocktail (Roche). Western blotting was performed after SDS-PAGE and transfer of the thereby separated proteins to Hybond PVDF membranes (GE Healthcare). After blocking the membranes in TBST (TBS containing 0.1% Tween 20) including 5% nonfat dry milk, they were incubated with different primary antibodies at a dilution of 1:1,000 at 4°C overnight. These were directed against phospho-Erk1/2 (#9101; Cell Signaling Technology), Erk1/2 (#4695; Cell Signaling Technology), β-actin (#MAB1501; EMD Millipore), phospho-Lrp6 (#2568; Cell Signaling Technology), or phospho-β-catenin (#9561; Cell Signaling Technology), respectively. Washing Steps were performed with TBST. Secondary HRP-conjugated antibodies (Dako) were used at a dilution of 1:2,000. Image acquisition was performed using a gel photoscanner (Scanjet G4050; Hewlett Packard).

Primary osteoclasts

For osteoclastogenesis, the bone marrow was flushed out of the femora from 12-wk-old C57BL/6 mice with α-MEM containing 10% fetal bovine serum. Cells were plated at a density of 5×10^6 cells/ml and grown in α-MEM containing 10% fetal bovine serum and 10 nM 1,25 dihydroxyvitamin-D3. On the following day the medium was removed, and the remaining adherent cells were cultured for three further days, before M-CSF (Peprotech) and RANKL (Peprotech) were added to a final concentration of 20 ng/ml and 40 ng/ml, unless stated otherwise. LiCl, Wnt3a (#1324WN; R&D Systems) or Wnt5a (#645WN; R&D Systems) was added from the day of seeding until the day of analysis, unless stated otherwise. For TRAP staining, the cells were washed with PBS and then fixed for 5 min in cold methanol. After two washing steps with distilled water, the fixed cells were first dried for 2 min before they were subjected to the TRAP-specific substrate Naphthol AS-MX Phosphate (Sigma-Aldrich). For quantification of osteoclastogenesis we determined the number of TRAP-positive multinucleated cells per well. For Western blot analysis cells were treated at day 3 of differentiation with Wnt3a (#1324WN, 100 ng/ml; R&D Systems) and the Fzd8-CRD (#112-FZ; R&D Systems) for 30 min. To demonstrate that the inhibitory effect of Wnt3a on osteoclastogenesis is mediated in an Opg-independent manner, cells were differentiated in the presence of an Opg-neutralizing antibody (#AF459, 200 ng/ml; R&D Systems), as described previously (Glass et al., 2005). Alternatively, bone marrow cells were sorted by CD11b immunoaffinity (#130-049-601; Miltenyi Biotec) to purify CD11b-positive osteoclast progenitors as described previously (Schulze et al., 2011). In brief, bone marrow cells were suspended in buffer containing 5% BSA (#130-091-222, #130-091-376; Miltenyi Biotec) and incubated with CD11b MicroBeads (10 µl per 10^7 cells) at 4°C for 15 min. The cell mixture was then applied to the column in the prepared magnetic field, and CD11b-negtaive cells were eluted with buffer. The CD11b-positive fraction was released by removing the columns from the magnetic field.

Mice

Fzd8-deficient mice (C57BL/6 genetic background) were obtained from the Jackson Laboratory (#005804). Offspring from heterozygous matings was genotyped for the presence of the wild type (5′-GTAGTCCTCCAGGCAGATGGGCGTG-3′ and 5′-AGTGACCTCGCTCCTAGCCGCCTTG-3′) and mutant allele (5′-GACGTTGTTTGTCTTCAAGAAGCTTC-3′and 5′-AGTGACCTCGCTCCTAGCCGCCTTG-3′), respectively. Mice with loxP sites located in introns 1 and 6 of the *Ctnnb1* gene were obtained from the Jackson Laboratory (#004152) and crossed with *LysM-Cre* mice (provided by T.J. Jentsch, Max Planck Institute for Molecular Genetics, Berlin, Germany) to generate $Ctnnb1^{fl/fl}/LysM^{+/+}$ and $Ctnnb1^{fl/fl}/LysM^{+/cre}$ littermates for skeletal analysis. Specificity of recombination was assessed by genomic PCR using primers amplifying the floxed (5′-AAGGTAGAGTGATGAAAGTTGTT-3′ and 5′-CACCATGTCCTCTGTCTATTC-3′) and recombined allele (5′-AATCACAGGGACTTCCATACCAG-3′ and 5′-GCCCAGCCTTAGCCCAACT-3′), respectively.

Histological analysis

All mice received two injections of calcein 9 and 2 d before sacrifice. Dissected skeletons were fixed in 3.7% PBS-buffered formaldehyde for 18 h before they were stored in 80% ethanol. To perform non-decalcified histology, we dehydrated a part of the spine (vertebral bodies L1 to L4) in ascending alcohol concentrations, before they were embedded into methylmetacrylate. Using a Microtec rotation microtome (Techno-Med GmbH) we cut 4-µm-thick sections in the sagittal plane. The sections were subsequently stained by von Kossa/van Gieson (for static hisotmorphometry) and toluidine blue (for cellular histomorphometry) staining procedures (Albers et al., 2011). Whereas the latter staining is achieved by incubation of the sections with 1% toluidine blue solution (pH 4.5) for 30 min, the von Kossa/van Gieson is a multistep procedure staining mineralized bone matrix in black and non-mineralized osteoid in red. More specifically, after staining with 3% silver nitrate for 5 min and incubation in 5% sodium thiosulfate for 5 min, counterstaining with van Gieson solution (0.25% acid fuchsin, 0.5% nitric acid [conc], 10% glycerine, and picric acid to saturation) was performed for a further 20 min. Static and cellular histomorphometry was performed on toluidine blue–stained sections, whereas dynamic histomorphometry for determination of the bone formation rate was performed on nonstained sections. All histomorphometric measurements were performed using the OsteoMeasure histomorphometry system (Osteometrics Inc., USA) according to American Society for Bone and Mineral Research standards (Parfitt et al., 1987). Here we followed the manufacturer's instructions by labeling the mineralized and nonmineralized bone surfaces, marking osteoblasts and osteoclasts, or labeling the calcein bands on unstained 12-µm sections for dynamic histomorphometry. TRAP activity staining was performed on decalcified sections that were preincubated in 10 mM sodium tartrate dissolved in 40 mM acetate buffer (pH 5) and then stained with 0.1 mg/ml Naphthol AS-MX Phosphate (#N-5000;) in the same buffer, including 0.6 mg/ml Fast Red Violet LB salt (#F-3881; Sigma-Aldrich). Staining of hyaloid vessels was performed as described previously (Albers et al., 2011). In brief, eyeballs were fixed in 3.7% PBS-buffered formaldehyde for 18 h, then dehydrated in ascending alcohol concentrations and embedded into paraffin. Sections of 5 µm were cut and stained by the hematoxylin/eosin procedure. For quantification we determined the number of stained hyaloid vessels per section. All histological images were captured at room temperature using a microscope (Axioskop; Carl Zeiss) with a 1.25× (no medium, NA 0.035), 20× (no medium, NA 0.045), or 40× (no medium, NA 0.75) objective fitted with a camera (Axiocam; Carl Zeiss). Image acquisition was performed using Axiovision Software (Carl Zeiss).

Serum analysis

Serum concentrations of serotonin, bone-specific collagen degradation products (Crosslaps), Opg, and Rankl were quantified using antibody-based detection kits (#BA 10-0900, LDN; #AC-06F1, Immunodiagnostic Systems; #MOP00, R&D Systems; #MTR00, R&D Systems).

Statistical analysis

All data are presented as means ± SDs. Statistical analysis was performed using unpaired, two-tailed Student's *t* test. For the comparison of more than two means, ANOVA (IBM SPSS Statistics 20) was used. P-values <0.05 were considered statistically significant.

Online supplemental material

Fig. S1 shows that there is no persistence of hyaloid vessels in the eyeballs of *Fzd8*-deficient mice, and that circulating serotonin levels are unaffected by the *Fzd8* deficency. Fig. S2 shows the specificity of recombination

in *Ctnnb1*$^{fl/fl}$/*LysM*$^{+/cre}$ mice and that primary osteoblasts derived from these mice mineralize normally and respond to Wnt3a administration. Online supplemental material is available at http://www.jcb.org/cgi/content/full/jcb.201207142/DC1.

This work was supported by grants from the Deutsche Forschungsgemeinschaft (SCHI 504/5-1 and SCHI 504/5-2) within the transregional research group Mechanisms of Fracture Healing and Bone Regeneration in Osteoporosis.

None of the authors have a conflict of interest to disclose.

Submitted: 23 July 2012
Accepted: 14 January 2013

References

Albers, J., J. Schulze, F.T. Beil, M. Gebauer, A. Baranowsky, J. Keller, R.P. Marshall, K. Wintges, F.W. Friedrich, M. Priemel, et al. 2011. Control of bone formation by the serpentine receptor Frizzled-9. *J. Cell Biol.* 192:1057–1072. http://dx.doi.org/10.1083/jcb.201008012

Baron, R., G. Rawadi, and S. Roman-Roman. 2006. Wnt signaling: a key regulator of bone mass. *Curr. Top. Dev. Biol.* 76:103–127. http://dx.doi.org/10.1016/S0070-2153(06)76004-5

Boyden, L.M., J. Mao, J. Belsky, L. Mitzner, A. Farhi, M.A. Mitnick, D. Wu, K. Insogna, and R.P. Lifton. 2002. High bone density due to a mutation in LDL-receptor-related protein 5. *N. Engl. J. Med.* 346:1513–1521. http://dx.doi.org/10.1056/NEJMoa013444

Boyle, W.J., W.S. Simonet, and D.L. Lacey. 2003. Osteoclast differentiation and activation. *Nature*. 423:337–342. http://dx.doi.org/10.1038/nature01658

Brault, V., R. Moore, S. Kutsch, M. Ishibashi, D.H. Rowitch, A.P. McMahon, L. Sommer, O. Boussadia, and R. Kemler. 2001. Inactivation of the beta-catenin gene by Wnt1-Cre-mediated deletion results in dramatic brain malformation and failure of craniofacial development. *Development*. 128:1253–1264.

Bucay, N., I. Sarosi, C.R. Dunstan, S. Morony, J. Tarpley, C. Capparelli, S. Scully, H.L. Tan, W. Xu, D.L. Lacey, et al. 1998. osteoprotegerin-deficient mice develop early onset osteoporosis and arterial calcification. *Genes Dev.* 12:1260–1268. http://dx.doi.org/10.1101/gad.12.9.1260

Clausen, B.E., C. Burkhardt, W. Reith, R. Renkawitz, and I. Förster. 1999. Conditional gene targeting in macrophages and granulocytes using LysMcre mice. *Transgenic Res.* 8:265–277. http://dx.doi.org/10.1023/A:1008942828960

Clevers, H., and R. Nusse. 2012. Wnt/β-catenin signaling and disease. *Cell*. 149:1192–1205. http://dx.doi.org/10.1016/j.cell.2012.05.012

Cui, Y., P.J. Niziolek, B.T. MacDonald, C.R. Zylstra, N. Alenina, D.R. Robinson, Z. Zhong, S. Matthes, C.M. Jacobsen, R.A. Conlon, et al. 2011. Lrp5 functions in bone to regulate bone mass. *Nat. Med.* 17:684–691. http://dx.doi.org/10.1038/nm.2388

Dann, C.E., J.C. Hsieh, A. Rattner, D. Sharma, J. Nathans, and D.J. Leahy. 2001. Insights into Wnt binding and signalling from the structures of two Frizzled cysteine-rich domains. *Nature*. 412:86–90. http://dx.doi.org/10.1038/35083601

Day, T.F., X. Guo, L. Garrett-Beal, and Y. Yang. 2005. Wnt/beta-catenin signaling in mesenchymal progenitors controls osteoblast and chondrocyte differentiation during vertebrate skeletogenesis. *Dev. Cell*. 8:739–750. http://dx.doi.org/10.1016/j.devcel.2005.03.016

DeAlmeida, V.I., L. Miao, J.A. Ernst, H. Koeppen, P. Polakis, and B. Rubinfeld. 2007. The soluble wnt receptor Frizzled8CRD-hFc inhibits the growth of teratocarcinomas in vivo. *Cancer Res.* 67:5371–5379. http://dx.doi.org/10.1158/0008-5472.CAN-07-0266

Glass, D.A. II, P. Bialek, J.D. Ahn, M. Starbuck, M.S. Patel, H. Clevers, M.M. Taketo, F. Long, A.P. McMahon, R.A. Lang, and G. Karsenty. 2005. Canonical Wnt signaling in differentiated osteoblasts controls osteoclast differentiation. *Dev. Cell*. 8:751–764. http://dx.doi.org/10.1016/j.devcel.2005.02.017

Gong, Y., R.B. Slee, N. Fukai, G. Rawadi, S. Roman-Roman, A.M. Reginato, H. Wang, T. Cundy, F.H. Glorieux, D. Lev, et al; Osteoporosis-Pseudoglioma Syndrome Collaborative Group. 2001. LDL receptor-related protein 5 (LRP5) affects bone accrual and eye development. *Cell*. 107:513–523. http://dx.doi.org/10.1016/S0092-8674(01)00571-2

Harada, S., and G.A. Rodan. 2003. Control of osteoblast function and regulation of bone mass. *Nature*. 423:349–355. http://dx.doi.org/10.1038/nature01660

Heath, D.J., A.D. Chantry, C.H. Buckle, L. Coulton, J.D. Shaughnessy Jr., H.R. Evans, J.A. Snowden, D.R. Stover, K. Vanderkerken, and P.I. Croucher. 2009. Inhibiting Dickkopf-1 (Dkk1) removes suppression of bone formation and prevents the development of osteolytic bone disease in multiple myeloma. *J. Bone Miner. Res.* 24:425–436. http://dx.doi.org/10.1359/jbmr.081104

Hill, T.P., D. Später, M.M. Taketo, W. Birchmeier, and C. Hartmann. 2005. Canonical Wnt/beta-catenin signaling prevents osteoblasts from differentiating into chondrocytes. *Dev. Cell*. 8:727–738. http://dx.doi.org/10.1016/j.devcel.2005.02.013

Holmen, S.L., C.R. Zylstra, A. Mukherjee, R.E. Sigler, M.C. Faugere, M.L. Bouxsein, L. Deng, T.L. Clemens, and B.O. Williams. 2005. Essential role of beta-catenin in postnatal bone acquisition. *J. Biol. Chem.* 280:21162–21168. http://dx.doi.org/10.1074/jbc.M501900200

Kato, M., M.S. Patel, R. Levasseur, I. Lobov, B.H. Chang, D.A. Glass II, C. Hartmann, L. Li, T.H. Hwang, C.F. Brayton, et al. 2002. Cbfa1-independent decrease in osteoblast proliferation, osteopenia, and persistent embryonic eye vascularization in mice deficient in Lrp5, a Wnt coreceptor. *J. Cell Biol.* 157:303–314. http://dx.doi.org/10.1083/jcb.200201089

Kramer, I., C. Halleux, H. Keller, M. Pegurri, J.H. Gooi, P.B. Weber, J.Q. Feng, L.F. Bonewald, and M. Kneissel. 2010. Osteocyte Wnt/beta-catenin signaling is required for normal bone homeostasis. *Mol. Cell. Biol.* 30:3071–3085. http://dx.doi.org/10.1128/MCB.01428-09

Li, J., I. Sarosi, R.C. Cattley, J. Pretorius, F. Asuncion, M. Grisanti, S. Morony, S. Adamu, Z. Geng, W. Qiu, et al. 2006. Dkk1-mediated inhibition of Wnt signaling in bone results in osteopenia. *Bone*. 39:754–766. http://dx.doi.org/10.1016/j.bone.2006.03.017

Little, R.D., J.P. Carulli, R.G. Del Mastro, J. Dupuis, M. Osborne, C. Folz, S.P. Manning, P.M. Swain, S.C. Zhao, B. Eustace, et al. 2002. A mutation in the LDL receptor-related protein 5 gene results in the autosomal dominant high-bone-mass trait. *Am. J. Hum. Genet.* 70:11–19. http://dx.doi.org/10.1086/338450

Maeda, K., Y. Kobayashi, N. Udagawa, S. Uehara, A. Ishihara, T. Mizoguchi, Y. Kikuchi, I. Takada, S. Kato, S. Kani, et al. 2012. Wnt5a-Ror2 signaling between osteoblast-lineage cells and osteoclast precursors enhances osteoclastogenesis. *Nat. Med.* 18:405–412. http://dx.doi.org/10.1038/nm.2653

Otero, K., M. Shinohara, H. Zhao, M. Cella, S. Gilfillan, A. Colucci, R. Faccio, F.P. Ross, S.L. Teitelbaum, H. Takayanagi, and M. Colonna. 2012. TREM2 and β-catenin regulate bone homeostasis by controlling the rate of osteoclastogenesis. *J. Immunol.* 188:2612–2621. http://dx.doi.org/10.4049/jimmunol.1102836

Overington, J.P., B. Al-Lazikani, and A.L. Hopkins. 2006. How many drug targets are there? *Nat. Rev. Drug Discov.* 5:993–996. http://dx.doi.org/10.1038/nrd2199

Parfitt, A.M., M.K. Drezner, F.H. Glorieux, J.A. Kanis, H. Malluche, P.J. Meunier, S.M. Ott, and R.R. Recker; Report of the ASBMR Histomorphometry Nomenclature Committee. 1987. Bone histomorphometry: standardization of nomenclature, symbols, and units. *J. Bone Miner. Res.* 2:595–610. http://dx.doi.org/10.1002/jbmr.5650020617

Qiang, Y.W., J.D. Shaughnessy Jr., and S. Yaccoby. 2008. Wnt3a signaling within bone inhibits multiple myeloma bone disease and tumor growth. *Blood*. 112:374–382. http://dx.doi.org/10.1182/blood-2007-10-120253

Rachner, T.D., S. Khosla, and L.C. Hofbauer. 2011. Osteoporosis: now and the future. *Lancet*. 377:1276–1287. http://dx.doi.org/10.1016/S0140-6736(10)62349-5

Rachner, T.D., P. Hadji, and L.C. Hofbauer. 2012. Novel therapies in benign and malignant bone diseases. *Pharmacol. Ther.* 134:338–344. http://dx.doi.org/10.1016/j.pharmthera.2012.02.005

Schulte, G., and V. Bryja. 2007. The Frizzled family of unconventional G-protein-coupled receptors. *Trends Pharmacol. Sci.* 28:518–525. http://dx.doi.org/10.1016/j.tips.2007.09.001

Schulze, J., S. Seitz, H. Saito, M. Schneebauer, R.P. Marshall, A. Baranowsky, B. Busse, A.F. Schilling, F.W. Friedrich, J. Albers, et al. 2010. Negative regulation of bone formation by the transmembrane Wnt antagonist Kremen-2. *PLoS ONE*. 5:e10309. http://dx.doi.org/10.1371/journal.pone.0010309

Schulze, J., T. Bickert, F.T. Beil, M.M. Zaiss, J. Albers, K. Wintges, T. Streichert, K. Klaetschke, J. Keller, T.N. Hissnauer, et al. 2011. Interleukin-33 is expressed in differentiated osteoblasts and blocks osteoclast formation from bone marrow precursor cells. *J. Bone Miner. Res.* 26:704–717. http://dx.doi.org/10.1002/jbmr.269

Teitelbaum, S.L., and F.P. Ross. 2003. Genetic regulation of osteoclast development and function. *Nat. Rev. Genet.* 4:638–649. http://dx.doi.org/10.1038/nrg1122

Tian, E., F. Zhan, R. Walker, E. Rasmussen, Y. Ma, B. Barlogie, and J.D. Shaughnessy Jr. 2003. The role of the Wnt-signaling antagonist DKK1 in the development of osteolytic lesions in multiple myeloma. *N. Engl. J. Med.* 349:2483–2494. http://dx.doi.org/10.1056/NEJMoa030847

Wei, W., D. Zeve, J.M. Suh, X. Wang, Y. Du, J.E. Zerwekh, P.C. Dechow, J.M. Graff, and Y. Wan. 2011. Biphasic and dosage-dependent regulation of osteoclastogenesis by β-catenin. *Mol. Cell. Biol.* 31:4706–4719. http://dx.doi.org/10.1128/MCB.05980-11

Wise, A., K. Gearing, and S. Rees. 2002. Target validation of G-protein coupled receptors. *Drug Discov. Today*. 7:235–246. http://dx.doi.org/10.1016/S1359-6446(01)02131-6

Yaccoby, S., W. Ling, F. Zhan, R. Walker, B. Barlogie, and J.D. Shaughnessy Jr. 2007. Antibody-based inhibition of DKK1 suppresses tumor-induced bone resorption and multiple myeloma growth in vivo. *Blood*. 109:2106–2111. http://dx.doi.org/10.1182/blood-2006-09-047712

Yadav, V.K., J.H. Ryu, N. Suda, K.F. Tanaka, J.A. Gingrich, G. Schütz, F.H. Glorieux, C.Y. Chiang, J.D. Zajac, K.L. Insogna, et al. 2008. Lrp5 controls bone formation by inhibiting serotonin synthesis in the duodenum. *Cell*. 135:825–837. http://dx.doi.org/10.1016/j.cell.2008.09.059